

POLAR TRANSFORMATION OF 2D X-RAY DIFFRACTION PATTERNS AND THE EXPERIMENTAL VALIDATION OF THE hDIC TECHNIQUE



Fatih Uzun^{a,1}, Alexey I. Salimon^b, Eugene S. Statnik^b, Cyril Besnard^a, Jingwei Chen^a, Thomas Moxham^a, Enrico Salvati^a, Zifan Wang^a, Alexander M. Korsunsky^{a,b,2}

^aMBLEM, University of Oxford, Department of Engineering Science, Oxford, U.K.

^bSkolkovo Institute of Science and Technology, Moscow, Russia

¹fatihuzun@me.com, fatih.uzun@eng.ox.ac.uk

²Corresponding Author, alexander.korsunsky@eng.ox.ac.uk

Authors' Accepted Manuscript

Published version in *Measurement*

Volume 151, 2020, 107193

<https://doi.org/10.1016/j.measurement.2019.107193>

ABSTRACT

Deformation analysis in engineering materials and components is a subject of ongoing enquiry due to its importance for obtaining reliable prediction of strength and durability of structures and assemblies. Whilst optical methods deliver information about surface displacements, X-ray scattering methods have the capability to provide efficient assessment of crystal lattice distortion in the bulk of the component. The height Digital Image Correlation (hDIC) technique is an alternative to conventional digital image correlation that uses the out-of-plane surface height variations for the identification of triaxial deformations. In this study, the hDIC technique was used for the determination of displacements in an aluminium specimen after 3-point bending process that creates a complex deformation state that includes both axial displacements and rotations. The surface of the specimen was prepared for the analysis by electric discharge machining (EDM) technique that has minimal effect on material properties and produces random height profile well-suited for the aim of this study. Surface height variations were measured using deep focus microscopy and used instead of pixel intensity for correlation in the Digital Image Correlation (DIC) process. The distribution of total of elastic and plastic strains were also calculated by the evolutionary eigenstrain model using 2D X-Ray diffraction patterns processed according to the polar transformation method. The agreement between hDIC and polar XRD analyses allowed reliable cross-validation between these two techniques.

Keywords: The hDIC technique; Deep focus microscopy; X-Ray diffraction; Polar transformation; Evolutionary eigenstrain model

1. INTRODUCTION

After the introduction of digital image correlation (DIC) for the purpose of the determination of in-plane displacements by Parks [1], Chu et. al [2] used digital speckle patterns for experimental mechanics. The developed technique is widely used for analysing the deformations on 2D and 3D surfaces [3] that are difficult to investigate using classical experimental methods [4]. The height Digital Image Correlation (hDIC) technique was developed by Uzun and Korsunsky [5] for the determination of in-plane and out-of-plane deformations. Authors performed tensile test for *in situ* analysis of the method and showed that the proposed sub-pixel level correlation provides an accuracy of 99.89 % in terms of Pearson coefficient during the elastic deformation. The high sensitivity of this method allowed determination of large deformations by correlation of final state of deformation and reference condition without using intermediate steps.

Residual stress has a critical role on understanding the mechanism behind deformations and fatigue life of materials for engineering applications. Correlation techniques are able to determine surface deformations, but the strains obtained using correlation processes are the sum of elastic and plastic deformations. However, classical residual stress measurement techniques can only determine elastic strains by correlating the stress relaxations up to the equilibrium state using destructive processes like FIB-DIC [6], measuring the contour variations as a result of planar cuts [7] and determining distance between crystallographic planes using diffraction techniques [8,9].

Eigenstrain theory has been used for the determination of plastic deformations and stresses without the requirement of complex material properties [10]. The use of diffraction

measurements combined with eigenstrain theory in numerical models [11] allows mapping of elastic and plastic strains. Korsunsky [12] developed an analytical solution procedure that uses eigenstrain theory with X-Ray diffraction data for the reconstruction of bending residual stress, but this model requires careful definition of the boundaries of elastic range by the user. In this study, a smart model, that uses evolutionary algorithms to define the boundaries of elastic range in that analytical model, was developed to determine distribution of elastic and plastic strains corresponding to the X-Ray diffraction measurements. Experimental residual strains were calculated using the data that was processed using the polar transformation technique which was developed by Statnik et. al. [13]. Being an effective technique with low computational demand made polar transformation a preferred technique for the analysis of experimental X-Ray diffraction data with high number of patterns.

DIC was first introduced using low computation capacity during the 1980's [1,2] and proceeding studies on this method mostly focused on improving the performance while keeping the process computationally efficient using simplifying assumptions [14,15]. Studies focused on the development of efficient [16,17], fast [14,18] and accurate [19] DIC algorithms, however validation of correlation processes using a highly reliable experimental method is still missing.

Reliability of the hDIC technique was investigated using HS 30 6082 aluminium specimen. Accuracy of this technique was analysed previously [5] by investigating different stages of a tensile test process, but, in this study, it was aimed to create a more complex deformation state that include both axial displacements and rotations. For this purpose, 3-point bent aluminium specimens was prepared. Height intensities of undeformed reference and deformed target states were created using deep focus microscopy on the region of interest. The same

area was also scanned by X-Ray diffraction technique and 2D X-Ray patterns were combined with evolutionary eigenstrain model, after polar transformation, for the experimental determination of the total of elastic and plastic strains.

2. THE hDIC TECHNIQUE

The use of digitalized images microscopy to determine in-plane deformations [20–22] is a well-known process. Different than conventional DIC techniques, the hDIC technique uses surface profile obtained by using deep focus microscopy that allows calculation of out-of-plane deformations. The Alicona InfiniteFocus is an instrument that allows capturing surface profile corresponding to the roughness. In this study, this device was used for scanning the EDM cut surfaces.

The hDIC process starts with integer-pixel level cross-correlation of subsets, with dimension of $(2N + 1) \times (2N + 1)$, between reference and target conditions using the zero-mean normalised cross-correlation method which is formulated in Equation 1. In this equation C_i is the cross-correlation coefficient of i^{th} subset, $R(x, y)$ is the intensity of the pixel at coordinates (x, y) in the reference subset, $T(x', y')$ is the intensity of the pixel at coordinates (x', y') in the target subset, R_m is the mean intensity of the pixels in the reference subset and T_m is the mean intensity of the pixels in the target subset.

$$C_i = \frac{\sum (R(x, y) - R_m)(T(x', y') - T_m)}{\sqrt{\sum (R(x, y) - R_m)^2} \sqrt{\sum (T(x', y') - T_m)^2}} \quad (1)$$

Coordinates of matching pixels after the correlation process are calculated using Equation 2 where u and v are the displacements in x- and y-axes respectively.

$$x' = x + u(x, y) \quad (2a)$$

$$y' = y + v(x, y) \quad (2b)$$

Integer-pixel level cross-correlation process is followed by sub-pixel level correlation based on gradient descent optimization method which was invented by Cauchy [23]. For this purpose, pixel intensities from height information are defined by a surface function, $F_T(x', y')$, using bi-cubic interpolation scheme which is formulated in Equation 3 that allows calculation of pixel intensity in the target subset at the coordinates defined by (x', y') where $\omega_{i,j}$ is the coefficient of the pixel defined by the indices of i and j . Details of the hDIC process and formulation of the gradient descent method can be found in the study that introduces the hDIC technique [5] .

$$F_T(x', y') = \sum_{i=0}^3 \sum_{j=0}^3 \omega_{i,j} (x')^i (y')^j \quad (3)$$

3. THE EVOLUTIONARY EIGENSTRAIN MODEL

Eigenstrain theory has been used for the determination of volumetric deformations [10] and creep modelling to simulate post weld heat treatment [24]. Despite the fact that the use of eigenstrain theory eliminates the need for complex material properties, new parameters arise that needs to be determined carefully. In order to deal with this problem, the principles of artificial intelligence were applied to eigenstrain reconstruction process [25]. Analytical

models are appropriate for profile fitting applications, but similar difficulties are also available for them. Korsunsky [12] previously developed a variational eigenstrain analysis model that uses synchrotron diffraction measurements of elastic strain in a bent titanium alloy bar. The proposed model effectively reconstructs eigenstrain fields at different rates of sensitivity related to the order of basis functions used for the analysis. In this study, evolutionary algorithm was combined with that analytical model for the determination of boundaries of elastic range and coefficients of the truncated series of basis distributions in spite of linear optimization process which is not able to determine the limits of elastic range.

The variational eigenstrain analysis model is based on the principle of additivity of elastic and inelastic strains that is given in Equation 4 where ϵ is the total strain, ϵ^* is the eigenstrain and e is the elastic strain. This model assumes the total strain variation to be linear through the thickness based on the Kirchhoff's hypothesis of straight normals.

$$\epsilon = e + \epsilon^* \quad (4)$$

The unknown eigenstrain in tensile and compressive fields are determined using N number of truncated series of basis distributions given in Equation 5. In this equation, ϵ^{*T} and ϵ^{*C} are eigenstrains at tensile and compressive fields, x'' is the position of the experimental data, d^T and d^C are the boundaries of elastic field with tensile and compressive plastic fields and c_l^T and c_l^C are the coefficients of tensile and compressive fields. In this study, genetic algorithm was used to develop evolutionary eigenstrain model.

$$\epsilon^{*T} = \sum_{l=1}^N c_l^T (x'' - d^T)^l \quad (5a)$$

$$\varepsilon^{*C} = \sum_{l=1}^N c_l^C (x'' - d^C)^l \quad (5b)$$

The evolutionary process used in this model aims to determine the model coefficients and the boundary between elastic and plastic regions that minimize the difference between experimental measurements and model calculations. The fitness function of the evolutionary process is given in Equation 6 where e_n^E and e_n^M are strains determined by experimental measurements and model calculations respectively at measurement point n .

$$J = \sum_{n=1}^a (e_n^E - e_n^M)^2 \quad (6)$$

Basic genetic algorithms is composed of selection, crossover and mutation operators which are used in the evolutionary eigenstrain model. Evolution of model variables starts with creation of random population of variables. After the calculation of the fitness for each member, the member with best fitness function is selected as elite member which is directly transferred to the next population. Then, operators of genetic algorithm are applied to all members to create other members of the next population. The evolution process continues until no improvement of elite member is observed for a predetermined number of generations. Details of this well-known evolution process of genetic algorithms and related flowchart are not given for the sake of simplicity. They can be found in the previous studies [26,27].

4. POLAR TRANSFORMATION OF 2D X-RAY DIFFRACTION PATTERNS

Statnik et. al. introduced a new strain evaluation method using 2D X-Ray diffraction patterns [28]. Authors proposed a new method for the determination of residual strains based on geometric transformation of 2D diffraction patterns from cartesian to polar coordinate system with respect to the patterns centre as illustrated in Figure 1. This process allows visualisation of Debye-Scherrer rings on the radial-azimuthal contour plot and fitting the entire transformed intensity pattern with a sine function that allows determination of residual strain variation while improving efficiency of processing of 2D X-Ray diffraction patterns at less time when compared to caking method [29].

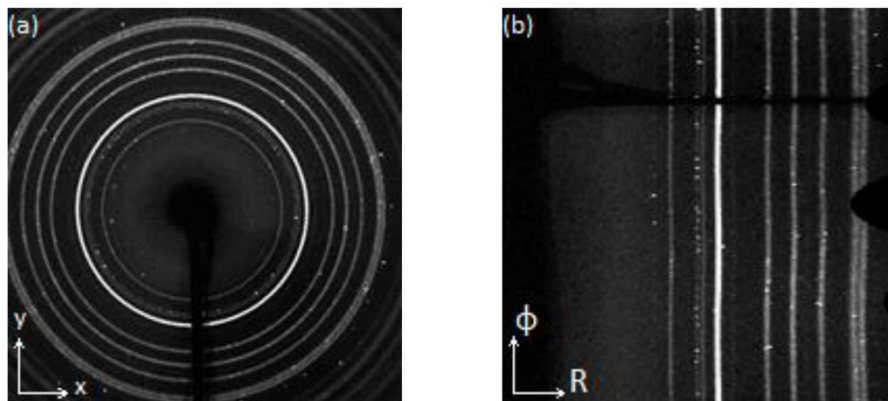


Figure 1. A typical 2D X-Ray diffraction pattern (a) and polar transformation of it (b) [28].

5. DEFORMATIONS AFTER 3-POINT BENDING

In-plane displacements on the surface of 3-point bent aluminium specimen were determined using the height intensities from the deep focus microscopy by scanning the surface of the specimen before and after the bending process. Deep focus microscopy images of reference and target conditions and corresponding height intensities and the region of interest are

illustrated in Figure 2. Longitudinal component of total strains was calculated using in-plane displacements.

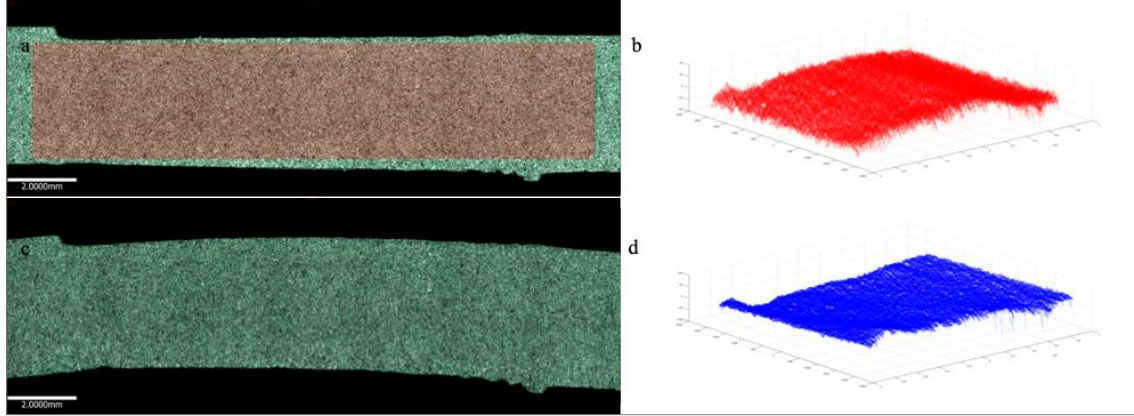


Figure 2. Microscopy images and surface profile of the reference (a) (b) and the target (c) (d) conditions of aluminium specimen.

After hDIC investigations, 2D X-Ray patterns were determined within the deformed aluminium specimen within an area that covers the region of interest. X-Ray measurements were performed at Diamond Light Source on the Test Beamline B16 using multi-layer monochromator at a beam energy of 18 keV. Strain calculations were performed using polar transformation method and longitudinal elastic strains were used in the evolutionary eigenstrain model to determine longitudinal component of total strains. Calculations on longitudinal component of total strains were compared with the total strains which were calculated using in-plane displacements for the validation of the hDIC technique.

The hDIC technique allows determination of triaxial deformations, but in this study, longitudinal x- and transversal y-components of in-plane surface displacements were calculated using this technique. Results of the correlation process are illustrated in Figure 3. Distribution of displacements as after 3-point bending shows high correspondence with

previous digital image correlations performed using digital images [30]. After obtaining the expected distribution of displacements, strain calculations for were performed using longitudinal x-component of displacements.

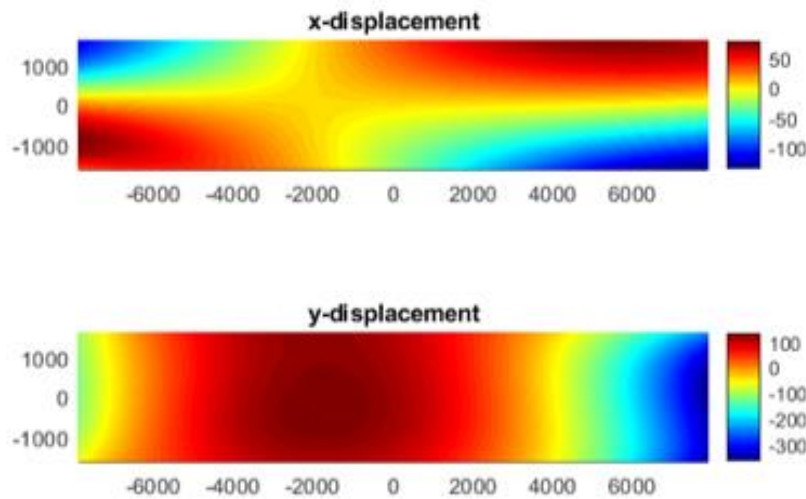


Figure 3. Longitudinal x- and transversal y-components of in-plane surface displacements (micron).

Results of the strain calculations, within the whole area covered in the region of interest, obtained using the hDIC and the polar transformation techniques are given in Figure 4. The hDIC technique allows calculation of total displacements and total strains while the polar transformation of 2D X-Ray patterns provides elastic strains. In order to have a better understanding on the deformations after the bending process, profile plots created using the data around the centre of the bent. Figure 3 shows that the centre of the bent is at about -1650 micron along the longitudinal direction that is located at left side of the centre of the region of interest. After careful investigation of the darkest red spot in the illustration for long

transverse y-component of displacement, profile plots of strains were created as the average of strains within the longitudinal region that expands from -500 to -2800 micron.

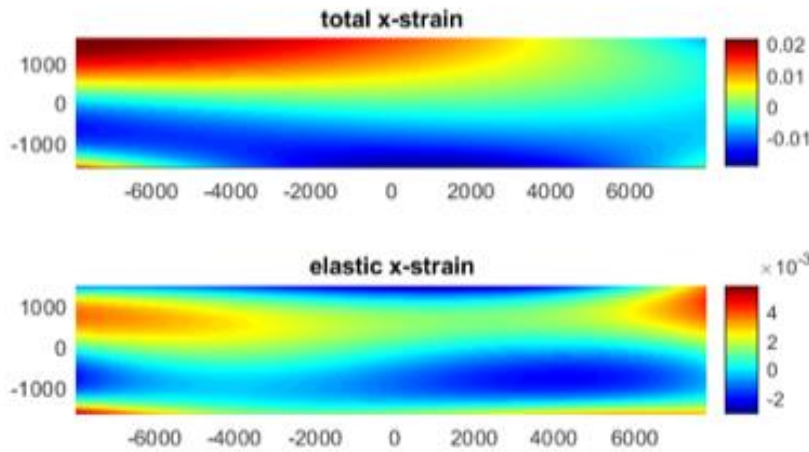


Figure 4. Distribution of longitudinal x-component of total strains calculated using the hDIC technique and elastic strains calculated using 2D X-Ray patterns.

Longitudinal x-component of elastic strains determined by polar transformation method were processed in the evolutionary eigenstrain model to calculate longitudinal x-component of total strains. This model fit the experimental residual strain values into a third order basis function and calculated both eigenstrains and total strains. Comparison of total strains calculated by the evolutionary eigenstrain model and the hDIC technique shows very good agreement in the elastic region as illustrated in Figure 5a. Figure 5b shows that eigenstrains in the elastic region are zero and the consistency between total strains determined by the hDIC technique and the evolutionary eigenstrain model is very high.

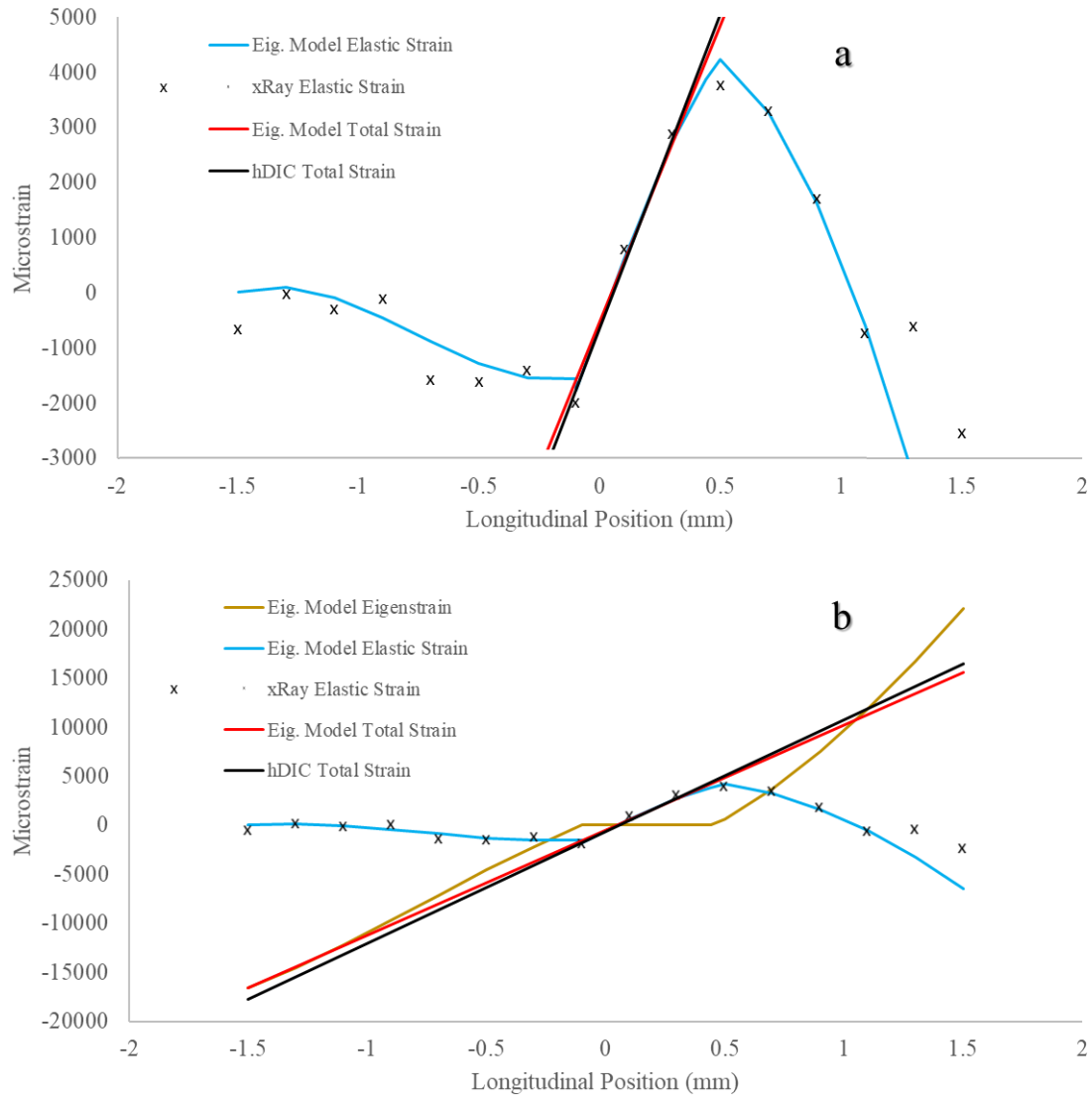


Figure 5. Comparison of the total strain calculations of the evolutionary eigenstrain model based on the experimental diffraction data, processed using polar transformation method, and the hDIC technique.

6. CONCLUSION

Polar transformation of 2D X-Ray patterns provided a novel approach on the determination of residual strain fields. This effective and fast method allowed the analysis of diffraction experiment data set with high number of 2D X-Ray patterns, for the purpose of mapping

elastic strain distribution, with low computation cost. The evolutionary eigenstrain method fit the experimental data from X-Ray patterns with third order basis functions and determined the distribution of total strains based on experimental data. Comparison of total strains calculated by the evolutionary eigenstrain model with the hDIC results showed almost perfect agreement. As a result of this study, it can be stated that the hDIC technique is validated by experimental X-Ray diffraction measurements and it is a reliable correlation technique for the determination of triaxial deformations.

ACKNOWLEDGEMENTS

This project has received funding from the European Union's Horizon 2020 research and innovation programme under the Marie Skłodowska-Curie grant agreement No 794957 and EPSRC through grant EP/S005072/1 Strategic Partnership in Computational Science for Advanced Simulation and Modelling of Engineering Systems (ASiMoV).

REFERENCES

- [1] V.J. Parks, The range of speckle metrology, *Exp. Mech.* 20 (1980) 181–191.
<https://doi.org/10.1007/BF02327597>.
- [2] T.C. Chu, W.F. Ranson, M.A. Sutton, Applications of digital-image-correlation techniques to experimental mechanics, *Exp. Mech.* 25 (1985) 232–244.
<https://doi.org/10.1007/BF02325092>.
- [3] P. Zhao, A.M. Zsaki, M.R. Nokken, Using digital image correlation to evaluate plastic shrinkage cracking in cement-based materials, *Constr. Build. Mater.* 182 (2018) 108–117. <https://doi.org/10.1016/j.conbuildmat.2018.05.239>.

- [4] F. Hild, S. Roux, Digital image correlation: From displacement measurement to identification of elastic properties - A review, *Strain*. 42 (2006) 69–80.
<https://doi.org/10.1111/j.1475-1305.2006.00258.x>.
- [5] F. Uzun, A.M. Korsunsky, The Height Digital Image Correlation (Hdic) Technique For The Identification Of Triaxial Surface Deformations, *Int. J. Mech. Sci.* 159 (2019) 417–423. <https://doi.org/10.1016/j.ijmecsci.2019.06.014>.
- [6] J. Everaerts, E. Salvati, F. Uzun, L. Romano Brandt, H. Zhang, A.M. Korsunsky, Separating macro- (Type I) and micro- (Type II+III) residual stresses by ring-core FIB-DIC milling and eigenstrain modelling of a plastically bent titanium alloy bar, *Acta Mater.* 156 (2018) 43–51. <https://doi.org/10.1016/j.actamat.2018.06.035>.
- [7] M.E. Kartal, Y.H. Kang, A.M. Korsunsky, A.C.F.F. Cocks, J.P. Bouchard, The influence of welding procedure and plate geometry on residual stresses in thick components, *Int. J. Solids Struct.* 80 (2016) 420–429.
<https://doi.org/10.1016/j.ijsolstr.2015.10.001>.
- [8] M. Kartal, M. Turski, G. Johnson, M.E. Fitzpatrick, S. Gungor, P.J. Withers, L. Edwards, Residual stress measurements in single and multi-pass groove weld specimens using neutron diffraction and the contour method, *Mater. Sci. Forum.* 524–525 (2006) 671–676. <https://doi.org/10.4028/www.scientific.net/MSF.524-525.671>.
- [9] M.B. Toparli, M.E. Fitzpatrick, S. Gungor, Improvement of the Contour Method for Measurement of Near-Surface Residual Stresses from Laser Peening, *Exp. Mech.* 53 (2013) 1705–1718. <https://doi.org/10.1007/s11340-013-9766-x>.
- [10] F. Uzun, A.M. Korsunsky, On the identification of eigenstrain sources of welding residual stress in bead-on-plate inconel 740H specimens, *Int. J. Mech. Sci.* 145 (2018) 231–245. <https://doi.org/doi.org/10.1016/j.ijmecsci.2018.07.007>.
- [11] E. Salvati, T. Sui, A.J.G. Lunt, A.M. Korsunsky, The effect of eigenstrain induced by

- ion beam damage on the apparent strain relief in FIB-DIC residual stress evaluation, *Mater. Des.* 92 (2016) 649–658. <https://doi.org/10.1016/j.matdes.2015.12.015>.
- [12] A.M. Korsunsky, Variational Eigenstrain Analysis of Synchrotron Diffraction Measurements of Residual Elastic Strain in a Bent Titanium Alloy Bar, *J. Mech. Mater. Struct.* 1 (2006) 259–277.
- [13] E.S. Statnik, A.I. Salimon, F. Uzun, A.M. Korsunsky, Polar Transformation of 2D X-ray Diffraction Patterns for 2D Strain Evaluation, in: *Proc. World Congr. Eng.* 2019, London, 2019.
- [14] B. Pan, K. Li, A fast digital image correlation method for deformation measurement, *Opt. Lasers Eng.* 49 (2011) 841–847. <https://doi.org/10.1016/j.optlaseng.2011.02.023>.
- [15] B. Wang, B. Pan, Subset-based local vs. finite element-based global digital image correlation: A comparison study, *Theor. Appl. Mech. Lett.* 6 (2016) 200–208. <https://doi.org/10.1016/j.taml.2016.08.003>.
- [16] F. Zhong, C. Quan, Efficient digital image correlation using gradient orientation, *Opt. Laser Technol.* 106 (2018) 417–426. <https://doi.org/10.1016/j.optlastec.2018.04.024>.
- [17] F.Q. Zhong, P.P. Indurkar, C.G. Quan, Three-dimensional digital image correlation with improved efficiency and accuracy, *Meas. J. Int. Meas. Confed.* 128 (2018) 23–33. <https://doi.org/10.1016/j.measurement.2018.06.022>.
- [18] H.S. Stone, M.T. Orchard, E.C. Chang, S.A. Martucci, A fast direct Fourier-based algorithm for subpixel registration of images, *IEEE Trans. Geosci. Remote Sens.* 39 (2001) 2235–2243. <https://doi.org/10.1109/36.957286>.
- [19] L. Zhang, T. Wang, Z. Jiang, Q. Kemao, Y. Liu, Z. Liu, L. Tang, S. Dong, High accuracy digital image correlation powered by GPU-based parallel computing, *Opt. Lasers Eng.* 69 (2015) 7–12. <https://doi.org/10.1016/j.optlaseng.2015.01.012>.
- [20] M. Sutton, C. Mingqi, W. Peters, Y. Chao, S. McNeill, Application of an optimized

- digital correlation method to planar deformation analysis, *Image Vis. Comput.* 4 (1986) 143–150. [https://doi.org/10.1016/0262-8856\(86\)90057-0](https://doi.org/10.1016/0262-8856(86)90057-0).
- [21] Z. Sun, J.S. Lyons, S.R. McNeill, Measuring Microscopic Deformations with Digital Image Correlation, *Opt. Lasers Eng.* 27 (1997) 409–428. [https://doi.org/10.1016/S0143-8166\(96\)00041-3](https://doi.org/10.1016/S0143-8166(96)00041-3).
- [22] M. Luo, Displacement/strain measurements using an optical microscope and digital image correlation, *Opt. Eng.* 45 (2006) 033605. <https://doi.org/10.1117/1.2182108>.
- [23] A.-L. Cauchy, Methode generale pour la resolution des systemes d'equations simultanees, *Compte Rendu Des Seances L'Acad'emie Des Sci.* 25 (1847) 536–538.
- [24] F. Uzun, A.M. Korsunsky, On the analysis of post weld heat treatment residual stress relaxation in Inconel alloy 740H by combining the principles of artificial intelligence with the eigenstrain theory, *Mater. Sci. Eng. A.* 752 (2019) 180–191. <https://doi.org/10.1016/j.finel.2018.11.004>.
- [25] F. Uzun, A.M. Korsunsky, On the application of principles of artificial intelligence for eigenstrain reconstruction of volumetric residual stresses in non-uniform Inconel alloy 740H weldments, *Finite Elem. Anal. Des.* 155 (2019) 43–51. <https://doi.org/10.1016/j.finel.2018.11.004>.
- [26] F. Uzun, Form-finding of free-form tensegrity structures by genetic algorithm-based total potential energy minimization, *Adv. Struct. Eng.* 20 (2017) 784–796. <https://doi.org/10.1177/1369433216664739>.
- [27] F. Uzun, Form-finding and analysis of an alternative tensegrity dome configuration, *Adv. Struct. Eng.* 20 (2017) 1644–1657. <https://doi.org/10.1177/1369433216689570>.
- [28] E.S. Statnik, A.I. Salimon, F. Uzun, A.M. Korsunsky, Polar Transformation of 2D X-ray Diffraction Patterns for 2D Strain Evaluation, (n.d.) 2–6.
- [29] J.E. Daniels, M. Drakopoulos, High-energy x-ray diffraction using the Pixium 4700

flat-panel detector, *J. Synchrotron Radiat.* 16 (2009) 463–468.

<https://doi.org/10.1107/S0909049509015519>.

- [30] A. Farsi, A.D. Pullen, J.P. Latham, J. Bowen, M. Carlsson, E.H. Stitt, M. Marigo, Full deflection profile calculation and Young ' s modulus optimisation for engineered high performance materials, *Nat. Publ. Gr.* 7 (2017) 1–13.

<https://doi.org/10.1038/srep46190>.